Journal of Thermal Analysis, Vol. 34 (1988) 1375–1385

A STUDY OF THE ELECTRICAL CONDUCTION AND DEVITRIFICATION BEHAVIOUR OF THE AMORPHOUS CHALCOGENIDE $Te_{81}Ge_{15}As_4$

M. F. Kotkata, H. H. Labib[+], *M. A. Afifi*[+] and *M. M. Abd El-Aziz*[+]

PHYSICS DEPARTMENT, FACULTY OF SCIENCE, AIN SHAMS UNIV., CAIRO
[+]PHYSICS DEPARTMENT, FACULTY OF EDUCATION, AIN SHAMS UNIV., CAIRO, EGYPT

(Received November 17, 1987)

The thermal spectrum of the *dc* conductivity of $Te_{81}Ge_{15}As_4$ during a consecutive heating-cooling cycle within the temperature range $T_g > T > T_m$ indicated that the heating and cooling parts of the cycle do not coincide and phase transformation were observed. The activation energies of conduction (ΔE) for the initial amorphous, the liquid and the final crystallized phases are 0.35, 0.30 and 0.16 eV, respectively. The growth of conductive regions during isothermal annealing of the amorphous solid phase was studied and correlated to the corresponding structural changes recorded by using microphotography and X-ray diffraction. The structure of the investigated three-component composition can be represented as a solid solution based on tellurium character. A value of 2.4 eV was obtained for the activation energy of crystallization from non-isothermal transition data.

Observations of switching in thin semiconducting films go back over a considerable period. Since Ovshinsky [1968] reported threshold processes in thin layers of chalcogenide glass alloys, there have been many attempts to explain these observations. Several investigators have maintained that the phenomena are essentially thermal, the current in the ON-state being carried by a hot filament. The switching phenomenon can be explained on the basis of two types of theories: (i) thermally initiated [1, 2] due to thermal instability, and (ii) electronically initiated [3–5] due to breakdown of the electronic equilibrium as a result of an applied field or current. Boer and Ovshinsky [2] have shown that the switching is initiated by a thermal process, followed by an electronic process. Buckley and Holmberg [6] have observed threshold switching in chalcogenide thin films in a sandwiched structure and concluded that switching is a bulk field effect. Little information is available in the literature on the switching phenomenon in bulk amorphous materials [7], and conclusions drawn from studies on thin films may not necessarily be applicable to bulk materials.

John Wiley & Sons, Limited, Chichester
Akadémiai Kiadó, Budapest

Glassy alloys in the system Te–Ge–As comprise an important class of amorphous semiconductors because of their ability to display memory switching [8–10]. Many workers have reported switching behaviour in thin films and/or in the bulk for different compositions in this ternary chalcogenide system. Previous studies on such materials indicate the dominant role of Te in the activation energy of the system.

Glass formation in the Te–Ge–As system contributes to the formation of complex three-component structural units with a considerable covalent component of the chemical bond, and also the formation of ternary eutectics [11]. One investigation [12] has shown that in the Te–Ge–As system there is a separate solid solution based on GeTe, GeAs, $GeAs_2$, As_2Te_3, As, Ge and Te.

The present work is aimed at a detailed investigation of the thermally induced structural transformation in one composition, namely $Te_{81}Ge_{15}As_4$, in the ternary chalcogenide system Te–Ge–As, which is frequently mentioned in the literature as a possible active material in threshold and memory switches.

Experimental methods

A glassy alloy of the composition $Te_{81}Ge_{15}As_4$ was prepared by heating a mixture of the elements [five nines purity) in vacuum (10^{-5} Torr) in a sealed fused silica ampoule in the following temperature steps: the temperature was raised from room temperature to 500° at 100 deg/h and kept at this temperature for 2 h, then increased to 900° at the same rate, and synthesis was continued in the rocking furnace for a long time (45 h) to ensure the homogeneity of the melt. The molten solution was then subjected to ice-water quenching. X-ray diffraction with a CuK_α source and differential thermal analysis [Shimazo Model DT–30] were used to verify the structural nature and homogeneity of the quenched ingot (10 g). Figure 1a shows the diffraction patterns, which is characterized by the absence of any diffraction lines, indicating the amorphous nature of the pepared material. The highest contribution of diffracting atomic planes in the domains of the crystalline sample (Fig. 1b) lies in the range of the low-angle halo of the amorphous pattern (Fig. 1a), which extends from about 20° to 40° in 2θ angular units.

Details of the experimental arrangement for DTA.and the microstructure were described elsewhere [13, 14].

Measurements of the electrical conductivity (σ) were carried out under vacuum (10^{-5} Torr) and in the dark. About 2 g from the prepared glass was crushed and placed in a dry clean silica ampoule (8 mm in diameter) provided with two coaxial tungsten electrodes near the base. To obtain good contact between the sample material and the electrodes, the tube was heated to a temperature $T = T_m + 50°$ for

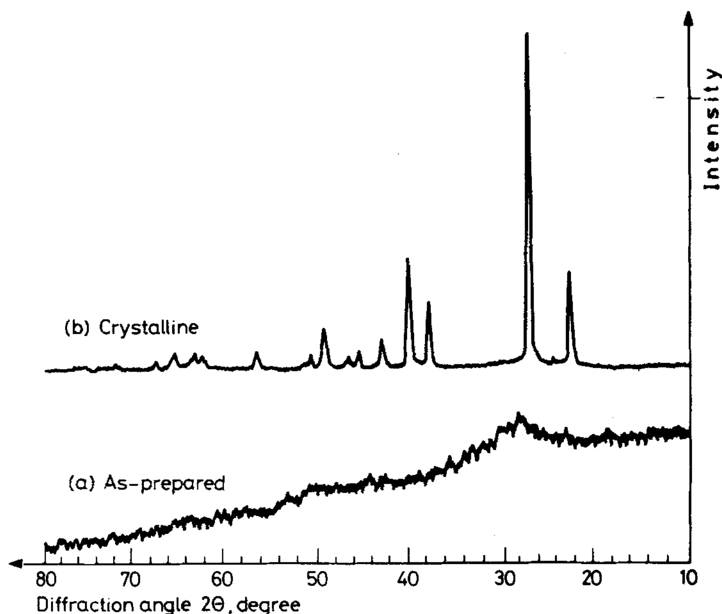

Fig. 1 X-ray diffraction patterns of (a) as-prepared and (b) crystalline samples of $Te_{81}Ge_{15}As_4$

1 h, then quenched in ice-water. A digital electrometer (Keithly 616) was used for the current measurements. The ohmic contact and reproducibility of the measurements were checked.

Results and discussion

Non-isothermal induced transition

Figure 2 shows typical DTA thermograms of $Te_{81}Ge_{15}As_4$, taken at different heating rates in the range 2–30 deg/min. The Figure illustrates three phenomena of interest: The glass transition (at temperature T_g), the crystallization exotherm (with maximum crystallization rate occurring at temperature T_c) and the melting endotherm (with melting point T_m). While T_m did not depend on the heating rate $\varnothing$ in the range 2–30 deg/min, and the dependence of T_g on the heating rate was slight (within $\pm 1°$), the crystallization exotherm location (begin–peak–end) changed markedly as $\varnothing$ was varied. The appearance of the endotherm due to the glass transition becomes clearer with increasing heating rate $\varnothing$. Further, the area under the crystallization peak becomes larger and shifts towards a higher temperature

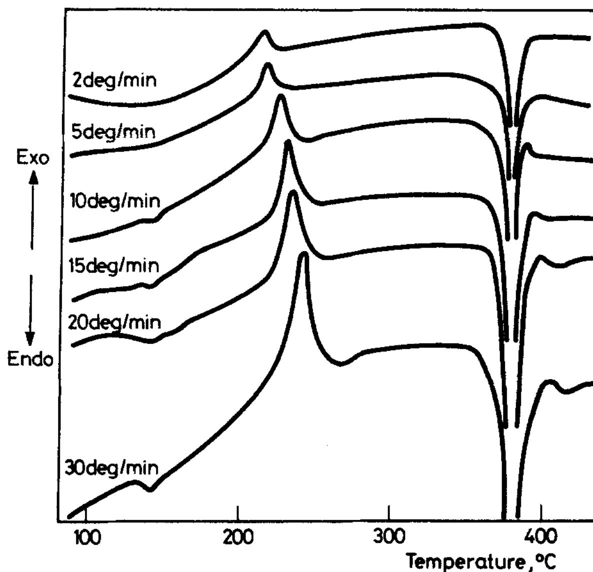

Fig. 2 DTA curves of amorphous $Te_{81}Ge_{15}As_4$ scanned at different rates

Table 1 Characteristic transition temperatures of $Te_{81}Ge_{15}As_4$ as a function of heating rate

Rate, Ø deg/min	T_g, °C	T, °C			T_m, °C	
		start	peak	end	start	peak
2	—	209	214	229	370	379
5	—	217	220	238	370	380
10	139	220	228	241	370	380
15	140	224	231	249	370	380
20	140	230	234	251	370	380
30	140	234	241	257	370	380

range with increasing Ø. Table 1 gives the characteristic transition temperatures T_g, T_c and T_m for the composition $Te_{81}Ge_{15}As_4$ at the different heating rates investigated.

Thermal spectrum of electrical conductivity

Figure 3 shows a typical thermal spectrum diagram for the electrical conductivity (σ) of the composition $Te_{81}Ge_{15}As_4$. Variation of the value of σ was recorded from room temperature up to about 500° during a consecutive heating—cooling cycle. Curve ABCDE follows the variation of σ during the heating process, and curve EFGH is the cooling path. The measurements were made with a small applied

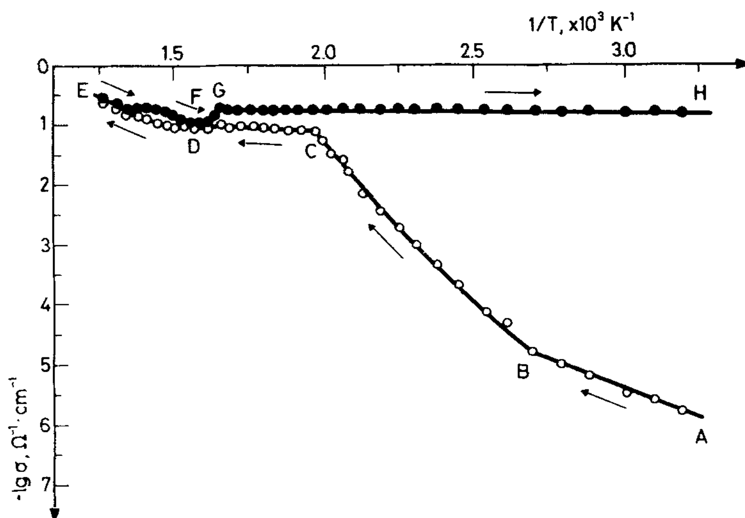

Fig. 3 Thermal spectrum of electrical conductivity of $Te_{81}Ge_{15}As_4$. Open circules denote, heating; full circles, cooling

stable voltabe (< 10 V). In the amorphous solid (AB), amorphous liquid (DE) and crystalline solid (FE) ranges, the measurements were made 30–45 minutes after attainment of the required temperature. In phase transition regions where σ changes rapidly with time, the measurements were made a few minutes after attainment of the required temperature. The temperature-dependence of σ in Fig. 3 indicates that the heating and cooling curves do not coincide. Accordingly, the thermal spectrum of conductivity shown in the Figure can be described as follows:

(i) Part A–B, which extends from room temperature up to point B ($\approx 100°$), represents linear semiconducting $\log \sigma$ vs. $1/T$ behaviour, in accordance with the thermal activation energy formula:

$$\sigma = \sigma_0 \exp[-\Delta E/K_B T]$$

In this formula, ΔE is the activation energy of the conduction process, K_B is Boltzmann's constant and T is the Kelvin temperature. For this glassy phase, $\Delta E = 0.35$ eV, the conductivity at 20° is $\sigma_{20} = 7.1 \times 10^{-7}$ ohm^{-1} cm^{-1} and the prefactor is $\sigma_0 = 1.58 \times 10^6$ ohm^{-1} cm^{-1}.

(ii) Part BCD, which extends from $\approx 100°$ up to $\approx 370°$, shows a rapid increase in σ. This may be attributed to crystallization from the amorphous phase. That is, the crystallization starts at point B and nearly comes to an end at point C (230°). Path C–D relates entirely to crystalline $Te_{81}Ge_{15}As_4$, which starts to melt at point D ($\approx 370°$). The observed small decrease in σ around point D is mainly due to liquefaction of a crystalline solid phase.

(iii) Part D–E is the linear dependence $\log \sigma$ *vs.* $1/T$, satisfying the above conductivity relation and defining the activation energy of conduction in the liquid phase, characterized by $\Delta E = 0.30$ eV and $\sigma_0 = 2.1 \times 10^5$ ohm^{-1} cm^{-1}. It is clear that there is a difference between the values of ΔE and σ_0 for the amorphous solid and the amorphous liquid (paths AB and DE). This may indicate that the mechanisms of conduction and liberation of free carriers are not exactly the same in the amorphous solid and amorphous liquid states.

(iv) Part E–G depicts a rather small variation of $\log \sigma$ *vs.* $1/T$, after point D indicating the possibility of the existence of a supercooled liquid phase at point G (330°).

(v) Part G–H shows a linear relationship $\log \sigma$ *vs.* $1/T$, characterizing crystallized $Te_{81}Ge_{15}As_4$ with $\Delta E = 0.06$ eV, $\sigma_{20} = 0.16$ ohm^{-1} cm^{-1} and $\sigma_0 = 2.2$ ohm^{-1} cm^{-1}.

Time-dependence of conductivity and microstructure

When an amorphous sample is subjected to isothermal annealing between T_g and T_m, a definite time is required for completion of the devitrification (crystallization) process. The latter, of course, depends on the temperature at which the crystal growth takes place.

Figure 4 shows the isothermal time-dependence of the *dc* conductivity of amorphous $Te_{81}Ge_{15}As_4$ annealed at 200°. Such a process of annealing leads to an increase in conductivity from about 3×10^{-6} ohm^{-1} cm^{-1} to about 4.5×10^{-3} ohm^{-1} cm^{-1} within 8 minutes. Increase of the annealing time does not lead to a pronounced change in the value of σ. The increase in σ is due mainly to the transformation of high-resistivity amorphous $Te_{81}Ge_{15}As_4$ into a rather better conducting (crystallized) state. This process is accompanied by a smooth liberation of heat energy, which is associated with the transition from a non-equilibrium thermodynamic state to a rather equilibrium one. That is, the growth stage is nearly finished after 8 minutes. The photomicrographs in Fig. 4 illustrate such growth stages at 200°. The crystallization process starts at small centres distributed in the amorphous medium. These centres gradually increase in size and become more ordered on increase of the annealing time.

Investigation of the isothermal time-dependence of the electrical conductivity of amorphous $Te_{81}Ge_{15}As_4$ at other temperatures, viz. 190° and 220°, reveals a similar behaviour to that in Fig. 4.

The variation in the extent of crystallization α with the annealing time can be computed from the empirical formula given by Landauer [15]:

$$\alpha = \frac{\log \sigma_t - \log \sigma_a}{\log \sigma_c - \log \sigma_a}$$

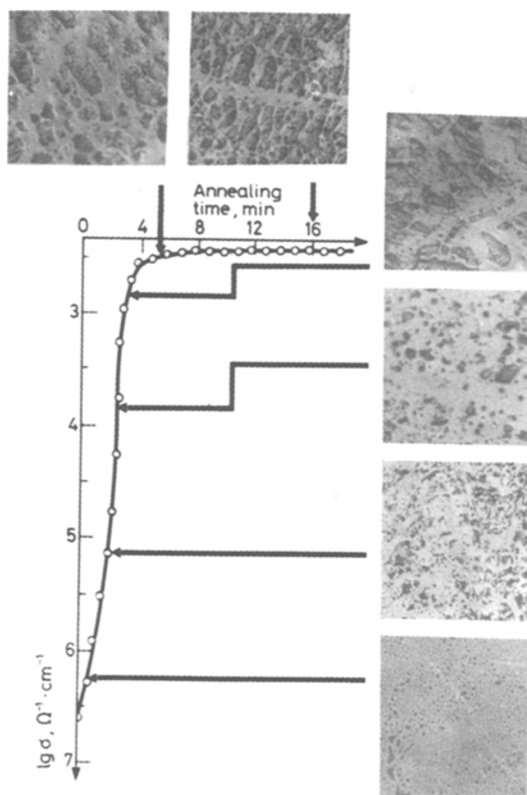

Fig. 4 Dependence of the electrical conductivity and the morphological changes on annealing time during isothermal transition of amorphous $Te_{81}Ge_{15}As_4$ at 200 °C

The subscripts *a* and *c* refer to values at the beginning and at the end of the transformation process, while the subscript *t* refers to a value at any time *t* between *a* and *c*.

Figure 5 shows the variation in the function $\alpha = f(t)$ for $Te_{81}Ge_{15}As_4$ annealed at 200°, together with the X-ray diffraction scans for a sample annealed for different times at 200°. After annealing for 3 minutes, four lines appeared, at d = 3.834, 3.175, 2.321 and 2.212 Å. Annealing for 6 minutes resulted in the appearance of three new lines, at d = 2.09, 2.014 and 1.831 Å. Annealing for 9 and 15 minutes each led to the appearance of one new line, at d = 1.814 Å and at d = 2.067 Å, respectively. The intensities of the lines increased and the relative half-widths of the peaks decreased with increase of the annealing time. The remaining diffraction lines characterizing the composition of $Te_{81}Ge_{15}As_4$ are shown in the pattern of the completely crystalline sample depicted in Fig. 1b.

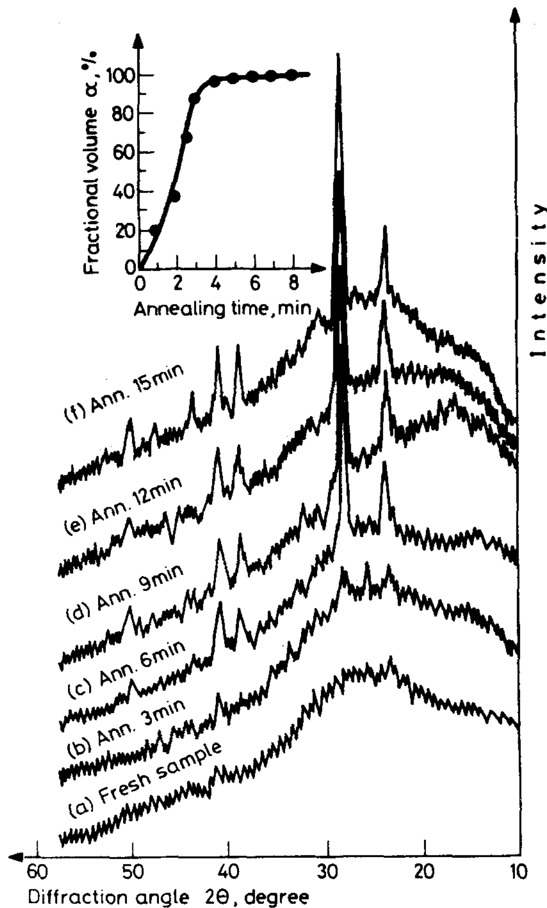

Fig. 5 X-ray diffraction patterns of amorphous $Te_{81}Ge_{15}As_4$ annealed at 200 °C for different soaking times. The inlet shows the time dependence of the fractional volume crystallized at 200 °C as calculated from the conductivity data of Fig. 4

A comparison of the data of the interplanar spacings (d_{hkl}) and their corresponding relative intensities (I/I_0) for the crystalline sample with those expected, given in the A.S.T.M. Diffraction Data File Index, indicates that the three highest lines, with d = 3.23, 2.34 and 2.22 Å, correspond to the diffraction lines of Te (hexagonal) [16]. The remaining diffraction lines of $Te_{81}Ge_{15}As_4$ also belong to Te, and no other phases are identified (Table 2). A comparison of the intensities of different lines indicates some preferred orientation of the planes.

Table 2 X-ray intensity I [arbitrary units] and interplanar spacing d [Å] for amorphous $Te_{81}Ge_{15}As_4$ crystallized for different annealing times at 200 °C

Annealing time										Crystalline		Te		[16]
3 min		6 min		9 min		12 min		15 min						
d, Å	*I*	*d*, Å	*I*	*d*, Å	*I*	*d*, Å	*I*	*d*, Å	*I*	*d*, Å	I/I_0	*d*, Å	I/I_0	*hkl*
3.834	1.4	3.802	2.7	3.802	3.1	3.802	3.2	3.818	3.4	3.866	30	3.348	25	100
3.175	1.5	3.198	9.8	3.187	10.5	3.209	11	3.209	13	3.23	100	3.245	100	101
2.321	0.4	2.327	1.6	2.332	2.2	2.327	2.4	2.322	3	2.34	19	2.347	35	102
2.212	0.6	2.212	2.3	2.227	2.3	2.217	2.4	2.217	3.5	2.22	33	2.221	29	110
–	–	2.09	0.6	2.076	0.7	–	—	2.076	1.6	2.085	9	2.081	9	111
–	–	2.014	0.3	2.049	1	2.058	0.5	2.067	1.4	1.969	4	1.972	12	003
–	–	1.831	0.5	1.907	0.7	1.949	1	1.914	1.1	1.926	2	1.924	5	200
–	–	–	–	1.814	1.3	1.814	1.1	1.817	1.8	1.838	11	1 835	16	201
										1.781	3	1.774	5	112
										1.621	4	1.616	8	202
										1.616	3	1.478	8	113

Effective activation energy of crystallization

The shift in the exothermic peak temperature with change of the heating rate, observed in Fig. 2, is used to determine the effective activation energy of the crystallization of $Te_{81}Ge_{15}As_4$. The peak temperature T_p is related to the heating rate $\varnothing$ by the relation [17]:

$$\frac{\mathrm{d}\ln[\varnothing/T_p^2]}{\mathrm{d}[1/T_p]} = -\frac{E_c}{R}$$

where R is the gas constant.

Figure 6 shows a plot of ln $(\varnothing/T_p^2)$ *vs.* $1/T_p$ (K^{-1}) for the crystallization exotherms of Fig. 2. A straight line was fitted to determine the effective activation energy E_c. The magnitude of E_c was found to be 2.4 eV.

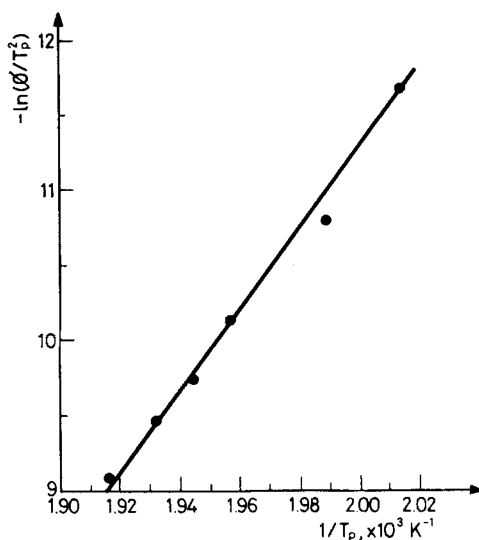

Fig. 6 Plot of ln $(\varnothing/T_p^2)$ *vs.* $(1/T_p)$ for amorphous $Te_{81}Ge_{15}As_4$

References

1 H. Fritzche and S. R. Ovshinsky, J. Non-Cryst. Solids, 4 (1970) 464.
2 K. W. Boer and S. R. Ovshinsky, J. Appl. Phys., 41 (1970) 2675.
3 N. F. Mott, Contemp. Phys., 10 (1969) 125.
4 M. Lida and A. Hamada, Japan J. Appl. Phys., 10 (1971) 224.
5 D. K. Reinhard, F. O. Arntz and D. Adler, Appl. Phys. Lett., 23 (1973) 521.
6 W. D. Buckley and S. H. Holmberg, Phys. Rev. Lett., 32 (1974) 1429.
7 K. Shimakawa, Y. Inagaki and T. Arizumi, Japan J. Appl. Phys., 12 (1973) 1043.

8 T. Matsushita, T. Yamagmi and M. Okuda, Japan J. Appl. Phys., 11 (1972) 923.
9 D. R. Goyal, O. S. Panwar and D. R. Ravikar, Indian J. Appl. Phys., 15 (1977) 10.
10 O. S. Panwar, A. Kumar and K. N. Lakshminarayan, J. Non-Cryst. Solids, 30 (1978) 37.
11 A. R. Hilton, C. E. Jones and M. Brau, Phys. Chem. Glasses, 7 (1966) 105.
12 G. Z. Vinogradova, S. A. Dembovskii, A. N. Kopeikina and N. P. Duzhnaya, Zh. Neorg. Khim., 20 (1975) 1367.
13 M. F. Kotkata and F. M. Ayad, J. Non-Cryst. Solide, 33 (1979) 13.
14 M. F. Kotkata, M. H. El-Fouly and M. A. Morsy, J. Thermal Anal., 32 (1987) 417.
15 R. Landauer, J. Appl. Phys., 23 (1952) 77.
16 Index to the Powder Diffraction File, A.S.T.M. Publications, Philadelphia, U.S.A. 1968, No. 4–0554.
17 H. E. Kissinger, J. Res. Nat. Bur. Stand., 47 (1956) 217.

Zusammenfassung — Das Thermospektrum der elektrischen Leitfähigkeit von $Te_{81}Ge_{15}As_4$ gegenüber Gleichstrom innerhalb eines konsekutiven Heiz-Kühlzyklus im Temperaturbereich $T_g > T > T_m$ zeigt ein Nichtzusammenfallen der Heiz- bzw. Kühlteile des Zyklus und Phasenumwandlungen wurden beobachtet. Die Aktivierungsenergien ΔE für die ursprüngliche amorphe, für die flüssige und die rekristallisierte Phase betragen 0,35, 0,30 bzw. 0,16 eV. Es wurde die Ausbeute leitfähiger Bezirke beim isothermen Tempern der amorphen Festphase untersucht und auf die korrespondierenden, mittels Mikrophotographie und Röntgendiffraktion beobachteten Strukturveränderungen bezogen. Die Struktur der untersuchten Dreikomponentenmischung kann als ein auf Tellurcharakter beruhendes Mischkristall angesehen werden. Für die Aktivierungsenergie der Kristallisation konnte aus nichtisothermen Messungen ein Wert von 2,4 eV bestimmt werden.

Резюме — Термический спектр *dc*-проводимости халькогенида $Te_{81}Ge_{15}As_4$ во время его последовательных циклов нагреб—охлаждение в температурном интервале $T_g > T > T_m$ показал несовпадение участков нагрева и охлаждения в пределах цикла и наличие фазового превращения. Энергии активации проводимости (ΔE) для исходной аморфной, жидкой и конечной кристаллической фазы, равнялись, соответственно, 0,35; 0,30 и 0,16 эв. Изучен рост проводящих участков во время изотермического охлаждения аморфной фазы, который коррелировался с соответствующими структурными изменениями, наблюдаемыми с помощью микрофотографии и рентгеноструктурного анализа. Структура трехкомпонентного состава может быть представлена в виде твердого раствора на основе теллура. На основе данных неизотермического перехода была найдена энергия активации процесса кристаллизации, равная 2,4 эв.